Indistinguishable MHz-narrow heralded photon pairs from a whispering gallery resonator

Sheng-Hsuan Huang ✉ 🔟 ; Thomas Dirmeier 🔟 ; Golnoush Shafiee; Kaisa Laiho 🔟 ; Dmitry V. Strekalov 🔟 ;
Andrea Aiello 🔟 ; Gerd Leuchs 🔟 ; Christoph Marquardt 🔟

Check for updates

View Online

Export Citation

Articles You May Be Interested In

On-chip heralded single photon sources

AVS Quantum Sci. (October 2020)

Heralded single-photon source fueled by light-emitting diode

Appl. Phys. Lett. (November 2019)

On-chip III-V monolithic integration of heralded single photon sources and beamsplitters

Appl. Phys. Lett. (February 2018)

Indistinguishable MHz-narrow heralded photon pairs from a whispering gallery resonator

View Online   Export Citation   CrossMark

Sheng-Hsuan Huang,[1,2,a)] (ID) Thomas Dirmeier,[1,2] (ID) Golnoush Shafiee,[1,2] Kaisa Laiho,[3] (ID)
Dmitry V. Strelalov,[2] (ID) Andrea Aiello,[2] (ID) Gerd Leuchs,[1,2] (ID) and Christoph Marquardt[1,2] (ID)

AFFILIATIONS

[1] Department of Physics, Friedrich-Alexander-Universität Erlangen-Nürnberg, Staudtstrasse 7/A3, 91058 Erlangen, Germany
[2] Max Planck Institute for the Science of Light, Staudtstrasse 2, 91058 Erlangen, Germany
[3] German Aerospace Center (DLR e.V.), Institute of Quantum Technologies, Wihelm-Runge-Str. 10, 89081 Ulm, Germany

[a)] Author to whom correspondence should be addressed: sheng-hsuan.huang@mpl.mpg.de

ABSTRACT

The Hong–Ou–Mandel interference plays a vital role in many quantum optical applications where indistinguishability of two photons is important. Such photon pairs are commonly generated as the signal and idler in the polarization-degenerate spontaneous parametric down-conversion (SPDC). To scale this approach to a larger number of photons, we demonstrate how two independent signal photons radiated into different spatial modes can be rendered conditionally indistinguishable by a heralding measurement performed on their respective idlers. We use the SPDC in a whispering gallery resonator, which is already proven to be versatile sources of quantum states. Its extreme conversion efficiency allowed us to perform our measurements with only 50 nW of in-coupled pump power in each propagation direction. The Hong–Ou–Mandel interference of two counterpropagating signal photons manifested itself in the fourfold coincidence rate, where the detection of two idler photons heralds a pair of signal photons with a desired temporal overlap. We achieved the Hong–Ou–Mandel dip contrast of 74% ± 5%. Importantly, the optical bandwidth of all involved photons is of the order of a MHz and is continuously tunable. This, on the one hand, makes it possible to achieve the necessary temporal measurement resolution with standard electronics and, on the other hand, creates a quantum state source compatible with other candidates for qubit implementation, such as optical transitions in solid-state or vaporous systems. We also discuss the possibility of generating photon pairs with similar temporal modes from two different whispering gallery resonators.

I. INTRODUCTION

The two-photon interference, named after Hong, Ou, and Mandel (HOM),[1] has attracted a great deal of attention since proposed in 1987. This intriguing effect, which does not have an analog in classical physics, plays a key role in many quantum applications, including boson sampling,[2] quantum communication,[3,4] and linear optical quantum computing.[5] In order to achieve the desired results, all these applications use beam splitter networks and quantum interference of several optical modes. This, in turn, requires the availability of indistinguishable photon pairs that can efficiently be interfered with each other. In addition to the ability to generate indistinguishable photons, the power consumption of the experiment should also be taken into account, as this may be a limiting factor for scalability.

In order to realize HOM interference between heralded states by fourfold coincidence discrimination, it is essential to generate two pairs of photons, which are indistinguishable in spatial, polarization, and temporal (frequency) modes. Several groups have demonstrated HOM interference via fourfold coincidence counting in previous experiments, including spontaneous parametric downconversion (SPDC) in χ^2 materials[6–8] and four-wave mixing (FWM) in on-chip ring resonators,[9,10] optical fibers,[11,12] and atomic systems.[13,14] On the one hand, SPDC is, at present, a commonly used method for generating quantum states because of its simplicity of operation and op-chip integration, which makes it favored in many experiments.

26 May 2025 18:55:10

However, the bandwidth of the generated SPDC photons is usually a few hundred GHz, which corresponds to temporal shapes having a width of a few femtoseconds. Considering the jitters of typical single photon detectors, which are usually larger that at least ten picoseconds, the temporal purity of the photons cannot be preserved in an experimental realization. Without knowledge of the temporal mode of the generated photons, it is not possible to achieve perfect mode matching for HOM interference, leading to a reduction in HOM visibility. On the other hand, the bandwidth of the generated photons from four-wave mixing in atomic systems can reach a value below 100 MHz in certain experimental arrangements such that the temporal purity can be preserved. However, the tunability of FWM systems is limited to comparatively narrow frequency window around the pump frequency and is strongly dependent on the atomic vapor used in the particular experiment. In addition, all previous studies required lasers with at least several milliwatts of pump power, which may cause problems when scaling up the system. Therefore, photon sources with narrow bandwidth and low pump power are needed for realizing large-scale quantum optical applications.

The SPDC in Whispering Gallery Mode Resonators (WGMRs) has been demonstrated to be a promising source of photonic quantum states, including the generation of heralded single photon states,[15] squeezed states,[16] and polarization-entangled photon pairs.[17] Unlike SPDC in bulk crystals, the bandwidth of the SPDC photons generated from a WGMR is often smaller than 100 MHz, providing a sufficient temporal bandwidth that a commercial single photon detector can resolve. The light is trapped in WGMRs due to total internal reflection, so the WGMRs work for the whole transparency region of the material, and no special anti-reflection coating is needed. Due to the triply resonant system, the SPDC process is very efficient in WGMRs. The required pump powers are usually smaller than a μW. These features make the WGMRs attractive for large-scale quantum information processing as potential sources of quantum states of light.

In this work, we demonstrate, for the first time, HOM interference between heralded states from a WGMR by counting fourfold coincidences. The key requirement for observing the HOM effect is to generate two photons, which are indistinguishable in spatial, polarization, and temporal modes. In our case, two photon pairs are generated by coupling the pump beam along the clockwise (CW) and counterclockwise (CCW) directions into the same whispering gallery mode. Since these two counterpropagating beams share the same medium and the same resonant mode, the phase matching conditions are the same for both beams, which makes the two signal photons and the two idler photons generated from the CW and CCW beams identical and traveling in opposite directions. In this experiment, the highest measured fourfold coincidence dip visibility reaches a value of 74% ± 5%. The in-coupled pump power we used here is only 50 nW for each propagation direction. We also show that the HOM dip visibility changes when the peak value of the Glauber second-order correlation function, $g_{si}^{(2)}(0)$, between signal (s) and idler (i) varies, which is realized by varying the power of the pump laser, and it follows the prediction provided from Ref. 18. Our results show that a strong photon–pair correlation is necessary in order to achieve a high HOM dip visibility. Finally, we replace the WGMR with a new one made of the same material but with different dimensions and demonstrate that it is possible to match the temporal mode of the generated photons produced from two WGMRs.

II. METHODS

A. Experimental setup

The experimental setup is schematically shown in Fig. 1. The WGMR is made from a z-cut lithium niobate wafer doped with 5% MgO. The shape is the same as reported in Ref. 19, with a major radius $R \approx 0.7$ mm and a minor radius $r \approx 0.14$ mm. It is coarsely temperature stabilized at 90 °C by using a Peltier element and a temperature controller in order to achieve type-I non-critical phase matching. The wavelengths of the pump, signal, and idler are 532, 950, and 1209 nm, respectively. The pump laser we used is a continuous-wave laser and is coupled into the WGMR from the CW and CCW directions. The non-polarizing beam splitters located on the left side of the WGMR are used to detect the reflected whispering gallery mode spectrum. One of these detected signals is also used as the input signal for the Pound–Drever–Hall technique[20] in order to generate an error signal for further stabilizing the WGMR.[21] The x-cut LiNbO$_3$ prism is used as a selective coupler, which brings
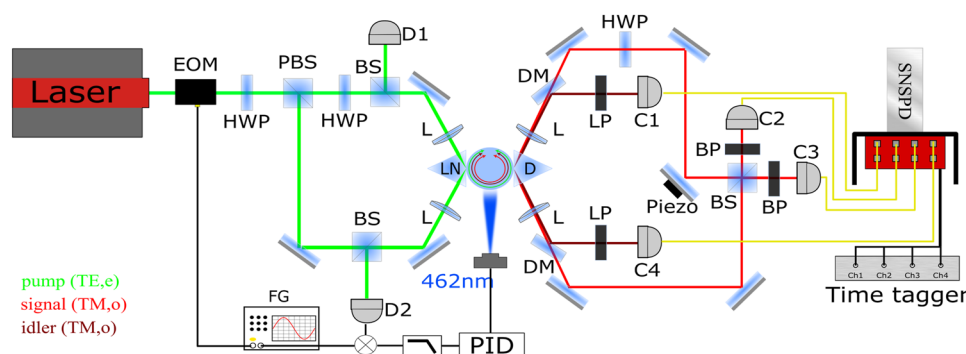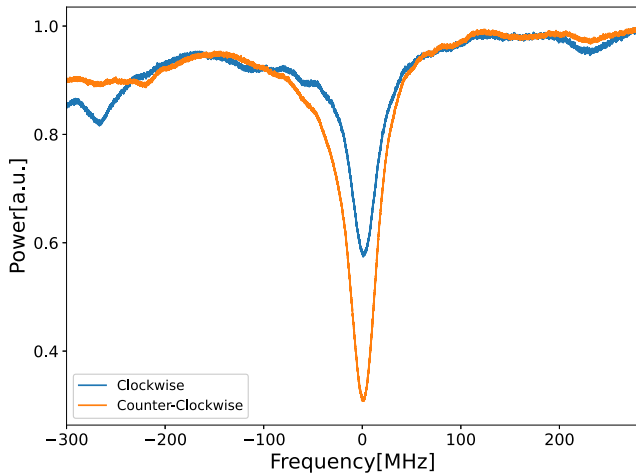

FIG. 1. Sketch of the experimental setup. EOM: electro-optic modulator, FG: function generator, HWP: half-wave plate, PBS: polarizing beam splitter, BS: non-polarizing beam splitter, PID: proportional–integral–derivative controller, LN: x-cut LiNbO$_3$ prism, D: diamond prism, DM: dichroic mirror, C1–C4: fiber couplers, LP: long pass filter, L: lens, D1–D2: photodetectors, BP: bandpass filter, SNSPD: superconducting nanowire single-photon detector, TM: transverse magnetic modes, TE: transverse electric field modes, o: ordinary, and e: extraordinary.

pump light into the resonator but forbids the signal and idler to be coupled out.[22] The diamond prism is used to couple the generated photons out of the WGMR. Then, the signals from both propagating directions are each guided to impinge on the input ports of a non-polarizing beam splitter such that the HOM interference can happen. After that, the light from the beam splitter output ports are coupled into two detectors. The idler beams are coupled to other two detectors separately and used as heralds. A fourfold coincidence is registered when the four detectors have clicked within given time windows.

B. Validating the similarity of heralded beams

To check whether the pump beams traveling in both directions are coupled to the same whispering gallery mode, we measure the reflected spectra from both directions. If the two pump beams are coupled to the same whispering gallery mode, the reflected spectra are the same. We show the results in Fig. 2. The reflected spectra have the same total linewidth of 38 MHz, resonate at the same frequency, and have a similar form, which confirms that the two beams occupy the same whispering gallery mode. The slight differences in the mode profiles and coupling efficiencies are due to imperfections in the optical components we used in our experiment. For example, the LiNbO$_3$ prisms we use here are not isosceles, so when we couple the light from both sides, we get different astigmatism, which results in different spectra and coupling efficiencies.

The spatial mode overlap and the polarization likeliness are optimized based on classical interference. To this end, we increase the pump power in order to drive our WGMR in the optical parametric oscillator (OPO) regime, where parametric photons are transformed into coherent light and the interference pattern on the signal beams' paths can be measured after combining the light from both directions on a non-polarizing beam splitter. Note that the phase locking between the CW and CCW signal modes responsible for the stationary interference fringe in Fig. 3 is not a trivial phenomenon. It is not expected for perfectly independent CW and CCW OPOs and is likely to originate from the backscattering of signals and idlers. By maximizing the visibility of the classical interference, the spatial-mode indistinguishability and polarization-mode indistinguishability are optimized as shown in Fig. 3. The highest visibility we achieved in this experiment is 86%. We measure the interference before coupling the beams into a single-mode fiber. The limiting factor comes mainly from the spatial mode distortion caused by the optical components we used. The visibility can be easily improved to almost unity if we measure the interference after coupling the beams into a single-mode fiber.

The similarity of the temporal modes between the counter-propagating heralded photons is confirmed by measuring the cross correlation functions in both directions. The results are shown in Fig. 4. The same values of $g_{si}^{(2)}(0)$ are achieved by adjusting the pump power of the CW and CCW processes. The bandwidth difference between the pump and signal (idler) wavelengths is due to several reasons. The pump and signal (idler) have different waveguide modes in the WGMR, the absorption coefficient of the crystal is wavelength dependent,[23] and the radial mode numbers of the pump, signal, and idler may be different. In addition, the local spectral environment can affect the bandwidth as well, via coupling to neighbor modes. We use a double exponential decay function to fit the results and use the fitted results to calculate the similarity between two cross correlation functions. The similarity S is defined as

$$S = \frac{\int_{t_c} f(x)g(x)\,dx}{\sqrt{\int_{t_c} f(x)^2\,dx \times \int_{t_c} g(x)^2\,dx}}, \qquad (1)$$
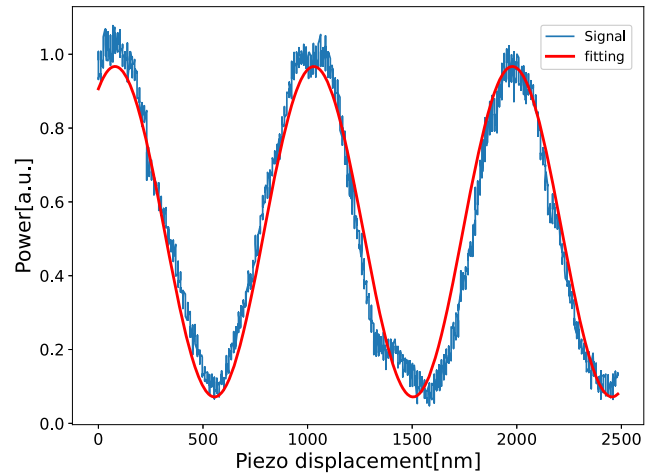
FIG. 2. Reflected pump spectra for the CW and CCW beams measured from D1 and D2, respectively. We use a wavemeter to measure the frequency sweep range of the pump laser and map it to the horizontal axis. The coupling efficiency is 25% for the CW and 50% for the CCW direction, which is calculated as $(P_{max} - P_{min})/(P_{max} + P_{min})$.

FIG. 3. Normalized interference pattern on the signal beams' paths in the OPO regime. The blue line is the experimental result, and the red line is the fitting result of a sinusoidal wave. The visibility is defined as $(P_{max} - P_{min})/(P_{max} + P_{min})$, which is 86% in this case.
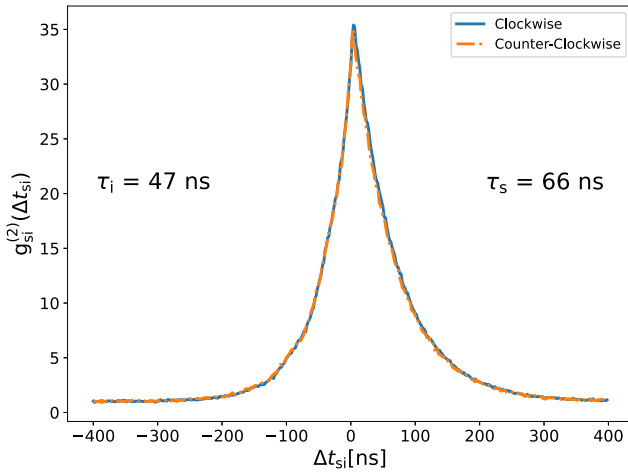
FIG. 4. Normalized second-order correlation functions taking the value $g_{si}^{(2)}(0)$ = 35. The decay time constants are 47 ns for the lead part and 66 ns for the tail part. The bandwidths of the signal and idler, calculated from the decay time constants, are 2.4 and 3.4 MHz, respectively. The difference is due to the difference of the linewidth between the signal and idler.[17]
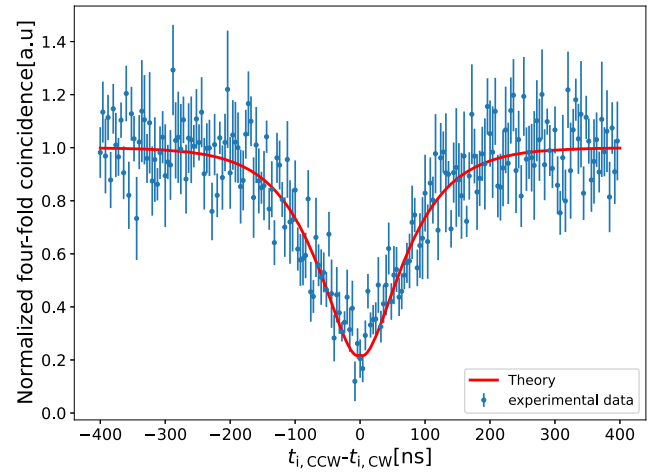
FIG. 5. Normalized HOM interference measured in 4 h. The values of $g_{si}^{(2)}(0)$ are 35 in both the CW and CCW directions. The red line presents the theoretical predication including the parameters extracted from Fig. 4. The errors are calculated assuming that the main uncertainties come from the photon counting statistics and that the statistics are Poissonian.

where t_c is the coherence time that is defined as the relative time at which $g_{si}^{(2)}(\Delta t_{si})$ decayed by $1/e^2$. For two identical functions, it is easy to see that the value S is equal to 1. In our experiment, the value S is 99.99%, showing that the temporal mode of the parametric photons between both propagating directions is well matched.

III. RESULTS

Figure 5 shows the investigated HOM interference and the theoretical prediction, which is calculated according to Ref. 18 with the photon spectrum taken from Ref. 24. See the supplementary material for details. We assume that the single round trip power loss in the crystal is negligible and the splitting ratio of the non-polarizing beam splitters is 0.5. The efficiencies on each beam path required for the model in Ref. 18 are estimated based on the experimental data. We record the fourfold coincidence dip with only 50 nW in-coupled pump power in each propagating direction. The fourfold coincidences are extracted with the following steps: First, we record all the events in which the two idler detectors click within time Δt. In order to observe the whole shape of the HOM interference dip, Δt should be larger than the photon coherence time. In our case, we choose Δt as ± 400 ns. We then look for the clicks of two signal detectors in a given coincidence window related to the coherence time of the signal and idler, each click corresponding to one of the idler detectors. From Fig. 4, we observe that the coincidence window is not symmetric but ranges from $-2\tau_i$ to $2\tau_s$. This measurement technique has advantages over the traditional HOM measurement when Δt is fixed by the beam splitter position, which needs to be varied in order to obtain an equivalent of Fig. 5. In our case, moving the beam splitter is not necessary and, in fact, would not be efficient, considering the long coherence length of the WGMR SPDC photons. Instead, all data points in Fig. 5 are recorded in a single measurement with a

fixed experimental setup and then postselectively sorted into a time series. The visibility of the HOM interference is defined as

$$V = \frac{C(\Delta t \to \infty) - C(\Delta t = 0)}{C(\Delta t \to \infty)}. \quad (2)$$

The visibility V gained from the results shown in Fig. 5 is 74% ± 5%. The visibility is mainly limited by the low $g_{si}^{(2)}(0)$ value. A low HOM visibility might limit scalability, but it can be easily addressed by increasing the value of $g_{si}^{(2)}(0)$. In our case, it can be increased by reducing the pump power or decreasing the distance between the coupling prisms and the resonator.[15]

In order to see the relation between $g_{si}^{(2)}(0)$ and the visibility of the HOM dip, we change the pump power to vary the value of $g_{si}^{(2)}(0)$. Figure 6 shows the experimental results and theoretical prediction, which agree nicely. One interesting point is that when $g_{si}^{(2)}(0) = 10$, the visibility of HOM interference is larger than the theoretical prediction. The reason for this is that the theoretical prediction is calculated assuming that the SPDC process is at the low-gain regime. This assumption works well at low pump powers. However, when the pump power increases [the value of $g_{si}^{(2)}(0)$ decreases], we are leaving the low-gain regime. Here, the in-coupled pump power is about 185 nW, while the OPO threshold is about 1 μW. In this case, this assumption does not hold, and therefore, the theoretical prediction does not work well for this data point.

Finally, we demonstrate that it is possible to match the temporal mode of heralded photons from different WGMRs by fabricating another resonator of different size using the same material and comparing the temporal mode with the resonator used above. The new resonator has a radius $R \approx 0.75$ mm with a rim radius $r \approx 0.14$ mm. We use the same 532 nm laser as the pump laser and tune the wavelength of the signal to 950 nm. In order to match the temporal mode,
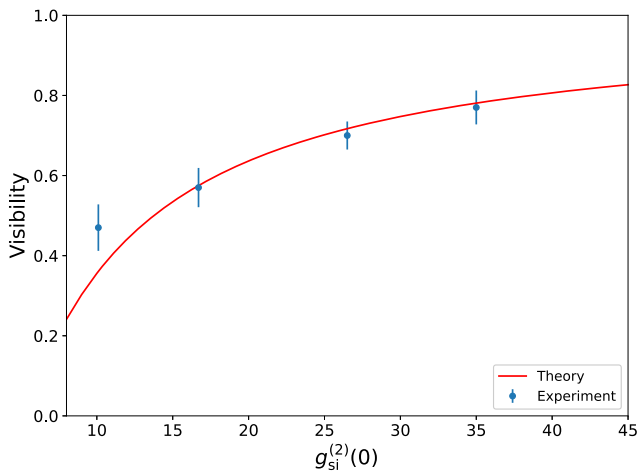
FIG. 6. Visibility of the HOM interference in terms of the peak value of the signal and idler cross correlation function. The errors are calculated assuming that the main uncertainties come from the photon counting statistics and that the statistics are Poissonian.

we vary the distance of the coupling prisms to change the bandwidths of SPDC photons.[15] The results of two temporal modes of heralded photons from two WGMRs are shown in Fig. 7. The similarity S between these two temporal modes is 99.97%, indicating that the temporal modes are well matched. Temporal profile matching is a key figure-of-merit when investigating the narrowband case, also delivering hints of the frequency characteristics. The polarization and spatial modes can be adjusted to match using standard optical components. Note that the frequency of generated photons has been shown to be continuously tunable by perturbing the evanescent field,[25] or by applying an electric field to the resonator.[26] These pave the way for an efficient HOM interference from different WGMRs, which is necessary for large-scale quantum applications.
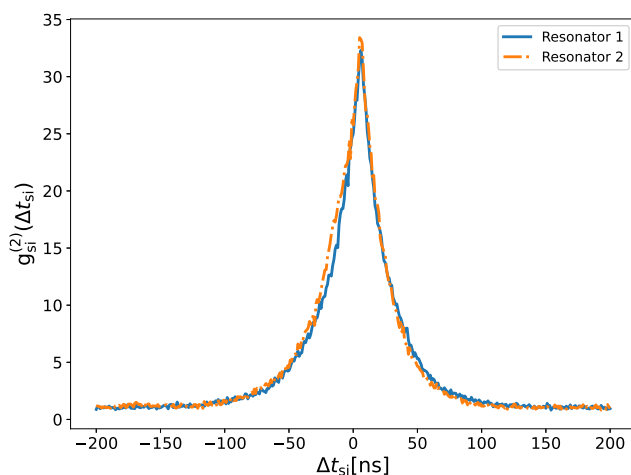
FIG. 7. Normalized second-order correlation functions from two WGMRs. Resonator 1 is the one we used for all measurements here, and resonator 2 is the new resonator.

IV. CONCLUSION

In conclusion, we have exploited the bidirectional pumping scheme to generate two pairs of indistinguishable photons in a WGMR and demonstrate the HOM interference between heralded states by counting fourfold coincidences. The highest visibility we achieve is 74% ± 5%. We experimentally show the relation between $g_{\text{si}}^{(2)}(0)$ and the visibility of the HOM interference. The results are consistent with the theoretical prediction in the low-gain regime. We also show that the temporal modes of the heralded photons from two WGMRs overlap very well, proving that it is possible to generate identical heralded photons from different WGMRs. Note that, although we use a continuous-wave laser here, we can also use a pulsed laser with proper parameters to pump the system.[27] In this case, we would have a natural clock to synchronize the different sources. Combining these with the ultra-low pump power requirement, we believe that WGMRs are promising platforms for realizing large-scale quantum information applications.

SUPPLEMENTARY MATERIAL

See the supplementary material for details on the derivation of the theoretical model used in this paper to calculate the HOM interference pattern.

ACKNOWLEDGMENTS

AUTHOR DECLARATIONS

Conflict of Interest

The authors have no conflicts to disclose.

Author Contributions

Sheng-Hsuan Huang: Conceptualization (equal); Data curation (equal); Formal analysis (equal); Investigation (lead); Methodology (equal); Software (equal); Validation (equal); Visualization (lead); Writing – original draft (equal); Writing – review & editing (equal). **Thomas Dirmeier**: Conceptualization (equal); Formal analysis (equal); Investigation (supporting); Methodology (equal); Software (equal); Validation (equal); Visualization (supporting); Writing – original draft (equal); Writing – review & editing (equal). **Golnoush Shafiee**: Conceptualization (equal); Investigation (supporting); Validation (equal); Writing – review & editing (equal). **Kaisa Laiho**: Conceptualization (equal); Methodology (equal); Validation (equal); Writing – original draft (equal); Writing – review & editing (equal). **Dmitry V. Strekalov**: Conceptualization (equal); Validation (equal); Writing – original draft (equal); Writing – review & editing (equal). **Andrea Aiello**: Methodology (equal);

Software (equal); Validation (equal); Writing – original draft (equal); Writing – review & editing (equal). **Gerd Leuchs**: Conceptualization (equal); Funding acquisition (equal); Supervision (equal); Validation (equal); Writing – review & editing (equal). **Christoph Marquardt**: Conceptualization (equal); Data curation (equal); Funding acquisition (equal); Supervision (equal); Validation (equal); Writing – original draft (equal); Writing – review & editing (equal).

DATA AVAILABILITY

The data that support the findings of this study are available from the corresponding author upon reasonable request.

REFERENCES

[1]C.-K. Hong, Z.-Y. Ou, and L. Mandel, "Measurement of subpicosecond time intervals between two photons by interference," Phys. Rev. Lett. **59**, 2044 (1987).

[2]D. J. Brod, E. F. Galvão, A. Crespi, R. Osellame, N. Spagnolo, and F. Sciarrino, "Photonic implementation of boson sampling: A review," Adv. Photonics **1**, 034001 (2019).

[3]X.-M. Hu, Y. Guo, B.-H. Liu, C.-F. Li, and G.-C. Guo, "Progress in quantum teleportation," Nat. Rev. Phys. **5**, 339–353 (2023).

[4]H.-K. Lo, M. Curty, and B. Qi, "Measurement-device-independent quantum key distribution," Phys. Rev. Lett. **108**, 130503 (2012).

[5]P. Kok, W. J. Munro, K. Nemoto, T. C. Ralph, J. P. Dowling, and G. J. Milburn, "Linear optical quantum computing with photonic qubits," Rev. Mod. Phys. **79**, 135–174 (2007).

[6]M. Halder, A. Beveratos, N. Gisin, V. Scarani, C. Simon, and H. Zbinden, "Entangling independent photons by time measurement," Nat. Phys. **3**, 692–695 (2007).

[7]P. J. Mosley, J. S. Lundeen, B. J. Smith, P. Wasylczyk, A. B. U'Ren, C. Silberhorn, and I. A. Walmsley, "Heralded generation of ultrafast single photons in pure quantum states," Phys. Rev. Lett. **100**, 133601 (2008).

[8]N. Bruno, A. Martin, T. Guerreiro, B. Sanguinetti, and R. T. Thew, "Pulsed source of spectrally uncorrelated and indistinguishable photons at telecom wavelengths," Opt. Express **22**, 17246–17253 (2014).

[9]I. I. Faruque, G. F. Sinclair, D. Bonneau, J. G. Rarity, and M. G. Thompson, "On-chip quantum interference with heralded photons from two independent microring resonator sources in silicon photonics," Opt. Express **26**, 20379–20395 (2018).

[10]PsiQuantum Team, "A manufacturable platform for photonic quantum computing," Nature (published online 2025).

[11]C. Söller, O. Cohen, B. J. Smith, I. A. Walmsley, and C. Silberhorn, "High-performance single-photon generation with commercial-grade optical fiber," Phys. Rev. A: At., Mol., Opt. Phys. **83**, 031806 (2011).

[12]M. Patel, J. B. Altepeter, Y.-P. Huang, N. N. Oza, and P. Kumar, "Independent telecom-fiber sources of quantum indistinguishable single photons," New J. Phys. **16**, 043019 (2014).

[13]P. Qian, Z. Gu, R. Cao, R. Wen, Z. Y. Ou, J. F. Chen, and W. Zhang, "Temporal purity and quantum interference of single photons from two independent cold atomic ensembles," Phys. Rev. Lett. **117**, 013602 (2016).

[14]T. Jeong, Y.-S. Lee, J. Park, H. Kim, and H. S. Moon, "Quantum interference between autonomous single-photon sources from Doppler-broadened atomic ensembles," Optica **4**, 1167–1170 (2017).

[15]M. Förtsch, J. U. Fürst, C. Wittmann, D. Strekalov, A. Aiello, M. V. Chekhova, C. Silberhorn, G. Leuchs, and C. Marquardt, "A versatile source of single photons for quantum information processing," Nat. Commun. **4**, 1818 (2013).

[16]A. Otterpohl, F. Sedlmeir, U. Vogl, T. Dirmeier, G. Shafiee, G. Schunk, D. V. Strekalov, H. G. L. Schwefel, T. Gehring, U. L. Andersen *et al.*, "Squeezed vacuum states from a whispering gallery mode resonator," Optica **6**, 1375–1380 (2019).

[17]S.-H. Huang, T. Dirmeier, G. Shafiee, K. Laiho, D. V. Strekalov, G. Leuchs, and C. Marquardt, "Polarization-entangled photons from a whispering gallery resonator," npj Quantum Inf. **10**, 85 (2024).

[18]K. Laiho, T. Dirmeier, G. Shafiee, and C. Marquardt, "Unfolding the Hong-Ou–Mandel interference between heralded photons from narrowband twin beams," New J. Phys. **25**, 083008 (2023).

[19]I. Breunig, B. Sturman, F. Sedlmeir, H. G. L. Schwefel, and K. Buse, "Whispering gallery modes at the rim of an axisymmetric optical resonator: Analytical versus numerical description and comparison with experiment," Opt. Express **21**, 30683–30692 (2013).

[20]E. D. Black, "An introduction to Pound–Drever–Hall laser frequency stabilization," Am. J. Phys. **69**, 79–87 (2001).

[21]G. Shafiee, D. V. Strekalov, A. Otterpohl, F. Sedlmeir, G. Schunk, U. Vogl, H. G. L. Schwefel, G. Leuchs, and C. Marquardt, "Nonlinear power dependence of the spectral properties of an optical parametric oscillator below threshold in the quantum regime," New J. Phys. **22**, 073045 (2020).

[22]F. Sedlmeir, M. R. Foreman, U. Vogl, R. Zeltner, G. Schunk, D. V. Strekalov, C. Marquardt, G. Leuchs, and H. G. L. Schwefel, "Polarization-selective out-coupling of whispering-gallery modes," Phys. Rev. Appl. **7**, 024029 (2017).

[23]M. Leidinger, S. Fieberg, N. Waasem, F. Kühnemann, K. Buse, and I. Breunig, "Comparative study on three highly sensitive absorption measurement techniques characterizing lithium niobate over its entire transparent spectral range," Opt. Express **23**, 21690–21705 (2015).

[24]C.-S. Chuu and S. E. Harris, "Ultrabright backward-wave biphoton source," Phys. Rev. A **83**, 061803 (2011).

[25]G. Schunk, U. Vogl, D. V. Strekalov, M. Förtsch, F. Sedlmeir, H. G. L. Schwefel, M. Göbelt, S. Christiansen, G. Leuchs, and C. Marquardt, "Interfacing transitions of different alkali atoms and telecom bands using one narrowband photon pair source," Optica **2**, 773–778 (2015).

[26]Y. Minet, S. J. Herr, I. Breunig, H. Zappe, and K. Buse, "Electro-optically tunable single-frequency lasing from neodymium-doped lithium niobate microresonators," Opt. Express **30**, 28335–28344 (2022).

[27]M. Förtsch, G. Schunk, J. U. Fürst, D. Strekalov, T. Gerrits, M. J. Stevens, F. Sedlmeir, H. G. L. Schwefel, S. W. Nam, G. Leuchs, and C. Marquardt, "Highly efficient generation of single-mode photon pairs from a crystalline whispering-gallery-mode resonator source," Phys. Rev. A **91**, 023812 (2015).